Water vapor and CMAS corrosion tests of Si/Y2SiO5 Thermal and Environmental Barrier Coating

Qi Zhang
Beijing Institute of Technology
Xueqin Zhang
Beijing Institute of Technology
Zhuang Ma
Beijing Institute of Technology
Ling Liu (richrad@bit.edu.cn)
Beijing Institute of Technology https://orcid.org/0000-0001-5926-7058
Yanbo Liu
Beijing Institute of Technology
Wei Zheng
Beijing Institute of Technology

Research Article

Keywords: thermal and environmental barrier coating, Y2SiO5 rare earth silicate, water vapor corrosion, CMAS corrosion

Posted Date: September 20th, 2021

DOI: https://doi.org/10.21203/rs.3.rs-889492/v1

Water vapor and CMAS corrosion tests of Si/Y_2SiO_5 thermal and environmental barrier coating

Qi Zhang [a,b], Xueqin Zhang [a,b], Zhuang Ma[a,b], Ling Liu[a,b*], Yanbo Liu[a,b], Wei Zheng[a]

[a] School of Materials Science and Engineering, Beijing Institute of Technology, Beijing 100081, China

[b] Beijing Institute of Technology Chongqing Innovation Center, Chongqing 401120, China

Abstract

Thermal and environmental barrier coating (TEBC), the up-to-date concept, is introduced to protect silicon-based ceramics matrix composites (CMC) from not only high temperature water vapor but also the alkali salt from volcanic ash and dust suspending in atmosphere. Because both of high temperature steam and CMAS will make Si-based CMC deteriorate rapidly. By executing the corrosion test against high temperature water vapor, we find that Si/Y_2SiO_5 double-layer TEBC can effectively protect SiC_f/SiC CMC from water vapor at 1300 ℃ for over 205 hours. Almost all Y_2SiO_5 transform into $Y_{4.67}(SiO_4)_3O$ after corrosion test. It is also found that in CMAS corrosion test, the reaction zone formed between CMAS and Y_2SiO_5 layer prevents the mutual diffusion of elements in CMAS and Y_2SiO_5 layer. The apparent activation energy of reaction between CMAS and Y_2SiO_5 in 1200~1300℃ temperature ranges is calculated to be 713.749kJ/mol. These findings provide a reference to select appropriate materials for TEBC.

Key words: thermal and environmental barrier coating, Y_2SiO_5 rare earth silicate, water vapor corrosion, CMAS corrosion

* corresponding author at: School of Materials Science and Engineering, Beijing Institute of Technology, Beijing 100081, PR China.

E-mail: L. Liu, richard@bit.edu.cn.

1. Introduction

In order to further develop the high thrust-weight ratio aero engine, decreasing the weight of ho section structural components and improving the inlet temperature of combustion room simultaneously is the most efficient approach[1]. Nickle-based high temperature alloy is used as the hot section structural materials in aero engine. However, the operating temperature in combustion room has already out of the usage temperature limit of the Ni-based alloy which restricts the further improvement of thrust-weight ratio. Si-based ceramics matrix composites (CMC) such as carbon fiber-reinforced silicon carbide CMC (C_f/SiC CMC) and silicon carbide fiber-reinforced silicon carbide CMC (SiC_f/SiC CMC) are promising candidates for hot section structural components due to low density and exceptional thermo-mechanical stability and good oxidation resistance[2-4]. In dry air, Si-based CMC will react with oxygen to form the silica which can isolate the oxygen and prevent Si-based CMC not to be oxidize further. However, the operating environment of Si-based CMC is full of hot gas containing high temperature water vapor. The passive silica will react with water vapor to form volatile $Si(OH)_4$[5]. The volatile $Si(OH)_4$ can be easily brushed away by high pressure hot gas, making Si-based CMC continuously exposure to hot gas. Continuous corrosion from water vapor makes Si-based CMC deteriorate rapidly.

The environmental barrier coating (EBC) fabricated on the surface of Si-based CMC aims at protecting Si-based CMC from hot gas at first. The EBC is always made up by two or three layers of coatings containing top layer and bond layer. The materials used as top layer of EBC should satisfy some constraints. For example, excellent water vapor corrosion resistance is the most fundamental condition. The coefficient of thermal expansion (CTE) of materials should be as close to the CTE of Si-based CMC as possible to avoid cracking and delamination of coating. Besides,

materials must be stable and compatible with bond layer so that deleterious reaction won't happen. The bond coating is deposited to alleviate the thermal mismatch between top layer and Si-based CMC resulting from the widely varying CTE between them. When oxygen permeating into coating along the cracks in top layer, the bond layer will consume oxygen and stop them continuously diffuse inward[6]. Over the past thirty years, researches about EBC have made great breakthrough. It has been proved that EBC effectively extends the service time of Si-based CMC [7]. The up-to-date EBC system containing rare earth silicate top layer and silicon bond layer is proved to be the most excellent candidate.

Researches have shown that resistance against high temperature water vapor of monosilicates is much more excellent than that of rare earth disilicates[6]. Besides, there are at most seven types of crystal structures of one disilicate over the wide temperature range[8,9]. The CTE of different crystal structures varies greatly which has an adverse influence on the integrality of EBC. There are only two types of crystal structures of every monosilicates[8,9]. So, the monosilicate is much more suitable to be used as top layer of EBC. Y_2SiO_5 is the most outstanding candidate out of many rare earth monosilicates due to its superior thermal and mechanical properties in high temperature condition[10-17]. The water vapor corrosion resistance of Y_2SiO_5 is also proved to be more excellent than other monosilicates from both experiments and simulated calculations[13-15].

The damage to Si-based CMC caused by high temperature water vapor can be alleviated through EBC as illustrated by several researches [14,18,19]. But Si-based CMC still faces the risk of corroded by foreign alkali salt. Foreign alkali salts will react with each other at high temperature to form the CMAS glass. CMAS can slowly permeate into the SiO_2 thin layer on the surface of Si-based CMC, destroying the

protection of SiO_2 for Si-based CMC. The Si-based CMC itself can be operated in extremely high temperature, so in addition to high temperature water vapor, the EBC only need protect Si-based CMC against CMAS, justly like the role of TBC to Ni-based alloy. And such thermal and environmental barrier coating (TEBC) is in urgent need[20]. However, most of researches only focus on the water vapor corrosion resistance of rare earth silicate. There is hardly any investigation about the resistance against the hot gas and CMAS simultaneously.

We deposited the Si/Y_2SiO_5 double layers TEBC on SiC_f/SiC substrate by air plasma spraying (APS) technique. The high temperature resistance against water vapor and CMAS of Si/Y_2SiO_5TEBC coatings were investigated. The corrosion behaviors and mechanisms were also discussed in detail.

2. Materials and methods

2.1 Deposition of coatings

The Y_2SiO_5 coating was deposited over the top of SiC_f/SiC composite substrates covered with silicon coating by air plasma spraying instrument (GTS-5500, Praxair, America) equipped with SG-100 spraying gun. The substrate used in the experiment was provided by Research Center of Composite Materials with the size of 17 mm×15 mm×3 mm. It is noticeable that when we purchased the substrates, the silicon coating with the thickness of 80 μm had already been fabricated on the surface of SiC_f/SiC composite substrates.

The Y_2SiO_5 powders used for top coating were obtained by spraying granulation and calcining with purchased Y_2SiO_5 powders (≥99.9%, 1-3μm, Beijing Zhongjinyan New Material Technology Co.,Ltd., Beijing, China). The slurry used in spraying granulation was a mixture of Y_2SiO_5 powders (35 wt.%), polyvinyl alcohol (PVA, 0.5 wt.%), and deionized water. After spray granulation, the Y_2SiO_5 powders were

calcined at 1100 ℃ in furnace to get rid of PVA and achieve the densification. The densified Y_2SiO_5 powders were sieved to obtain the spraying powders meeting the flowability required in APS process.

The Y_2SiO_5 coatings was deposited at room temperature. The thickness Y_2SiO_5 coatings was 120 μm, respectively. The substrate coated with silicon coating was ultrasonically cleaned in ethanol to keep the surface clean before coating deposition. The substrates were fixed on the steel wire gauze on the surface of steel shelf. The spraying parameters were shown in Table 1. The moving rate during coating deposition is 0.5 m/s. After deposition, the coatings were annealing in Ar atmosphere at 1400℃ to release the stress generated in preparing process. The Si/Y_2SiO_5 coated substrates were then ultrasonic cleaned in ethanol for further test.

Table 1 Plasma spraying parameters used for the deposition of Y_2SiO_5 coatings.

Parameter	Value
Spraying current (A)	800
Primary gas (Ar) flow (L min^{-1})	40
Secondary gas (He) flow (L • min^{-1})	14
Carrier gas (Ar) flow (L min^{-1})	4.7
Powder feed rate (RPM)	3.0
Spray distance (mm)	80

2.2 Water vapor corrosion test

Water vapor corrosion test of Si/Y_2SiO_5 coated SiC_f/SiC substrates at elevated temperature was carried out in tube furnace (GSL-1600X, Hefei Kejing Material Technology Co., Ltd.). The test was performed at 1300 ℃ in 90%H_2O/10%O_2 atmosphere on a 10-hour rotation. The gas generator (LVD-F1, Hefei Kejing Material

Technology Co., Ltd.) was used to generate the vapor and the flow rate of steam was 0.17 cm/s. In order to accurately obtain the weight change tendency of samples during water vapor corrosion process, the samples on the alumina boat were taken out from the tube furnace and measured the weight of the sample every 10 h.

2.3 CMAS corrosion test

The 38CaO-5MgO-8$AlO_{1.5}$-49SiO_2 (CMAS) was used as corrosive medium to simulate practical situation of aero-energy in service. The CMAS powders were grinded and uniformly coated on the surface of coating and then heated to 1200, 1250 and 1300 ℃ in furnace at a heating rate of 5 ℃/min for 15, 90, 150 and 240 min. The CMAS powders used in this work were synthesized at 1550℃ for 4 h with CaO, MgO, Al_2O_3 and SiO_2 in a molar ratio of 38:5:4:49. The CaO and Al_2O_3 powders (AR, 3-5 μm, Shanghai, China) were provided by Shanghai Aladdin Biochemical Technology Co.,Ltd. The MgO and SiO_2 powders (AR, 3-5 μm, Beijing, China) were both provided by Sinopharm Chemical Reagent Beijing Co.,Ltd.

2.4 Analysis and characterization

The morphologies of coatings before and after corrosion and the elements distribution were observed by scanning electron microscope (SEM, Philips S-4800, Hitachi Ltd., Yokohama, Japan) with attached energy dispersive spectrometer (EDS). The SEM can also be used to measure the thickness of emerging layer between Y_2SiO_5 and silicon layer after corroding. The phases compositions of coating in different states were characterized by X-ray diffractometer (XRD, RIGAKU D/Max-rB, Rigaku International Corp., Tokyo, Japan). The scanning rate of XRD test was 5 °/min over the 2θ range of 10°-90°.

3. Materials and Methods

3.1 Comparison of Si/Y_2SiO_5 TEBC before and after water oxygen corrosion

According to the weight change rule of Si/Y_2SiO_5 coated SiC_f/SiC substrate corroded in $90\%H_2O/10\%O_2$ atmosphere at 1300℃, it can be found that Si/Y_2SiO_5 can persistently protect SiC_f/SiC substrate from high temperature water vapor for more than 193 hours. The maximum weight gain per unit area is less than 0.4 mg/cm^2 throughout the whole corrosion test. In the initial stage of corrosion, there is slightly increase of weight per unit area. In the next few hours, the mass change versus time curve keeps flat without obvious fluctuation. The curve drops suddenly when accumulated corrosion time over 193 hours. The decline of mass change versus time curve can be attributed to the partly peeling off of Si/Y_2SiO_5 coating. In our pre-experiment, the mullite/Y_2SiO_5 TEBC system can only provide the protection for SiC_f/SiC substrate no more than 105 hours. The water vapor corrosion resistance of Si/Y_2SiO_5 is also apparently excellent than $ZrSiO_4$ coating[21]. The works mentioned above demonstrate Si/Y_2SiO_5 TEBC system has great potential against high temperature water vapor.

The surface microstructure of Si/Y_2SiO_5 TEBC before and after water vapor corrosion in $90\%H_2O/10\%O_2$ atmosphere at 1300 ℃ are shown in Fig. 1. It can be seen clearly from Fig. 1(a) that before high temperature water vapor corrosion, the top photography Y_2SiO_5 layer is relatively flat. Almost all Y_2SiO_5 powders melt and spread well. After 205 hours' corrosion test, there are obvious corrosive traces on the topography of Y_2SiO_5 layer accompanying with several cracks as shown in Fig. 1(b) and Fig. 1(c).

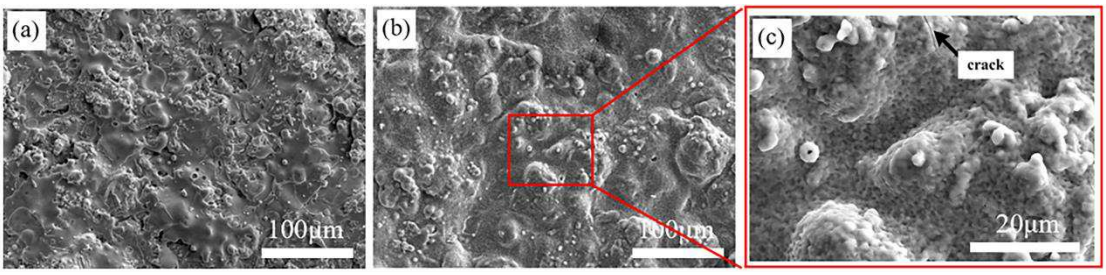

Fig. 1 Surface microstructure of Si/Y_2SiO_5 TEBC (a) before and (b) after corrosion in 90%H_2O/10%O_2 atmosphere at 1300 ℃, (c) magnification of (b)

The cross-section microstructure of Si/Y_2SiO_5 TEBC before and after water vapor corrosion are shown in Fig. 2. It can be seen from Fig. 2(a) that Si/Y_2SiO_5 TEBC before corrosion is dense without mud-cracks and large holes. The Y_2SiO_5 top layer combines Si bond layer well. The large area defect in Si bond coating is caused in sample making process by accident. After 205 hours' water vapor corrosion in 90%H_2O/10%O_2 atmosphere at 1300 ℃, the width of micro cracks gets larger and the number of micro holes gets bigger. The EDS analysis result demonstrates that the emerging layer between top layer and bond layer after corrosion is thermal growing oxide (TGO).

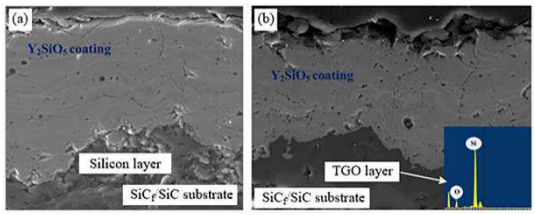

Fig. 2 Cross-section microstructure of Si/Y_2SiO_5 TEBC (a) before and (b) after corrosion in 90%H_2O/10%O_2 atmosphere at 1300 ℃

The phases detected by XRD before and after water vapor corrosion test are shown in Fig. 3. The main phase in coating before corrosion is Y_2SiO_5. There is also a small amount of $Y_{4.67}(SiO_4)_3O$ exists in coating. After corrosion test, the $Y_{4.67}(SiO_4)_3O$

accounts for the vast majority of coating and the amount of Y_2SiO_5 significantly decreases compare with the phase composition of coating before corrosion.

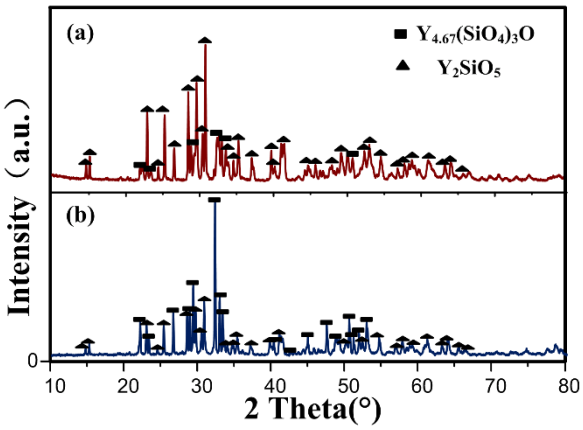

Fig. 3 Phase composition of Si/Y_2SiO_5 TEBC (a) before and (b) after corrosion in $90\%H_2O/10\%O_2$ atmosphere at 1300 ℃

3.2 Water vapor corrosion mechanism of Si/Y_2SiO_5 coatings

As depicted in Fig. 4(a), at early stage of water vapor corrosion test, the Y_2SiO_5 top layer keeps intact. There is almost no obvious defect on the surface and cross-section of coating. The Y_2SiO_5 top layer commendably protect bond layer and SiC_f/SiC substrate from high temperature water vapor so that there is only slightly weight gain at early stage of corrosion.

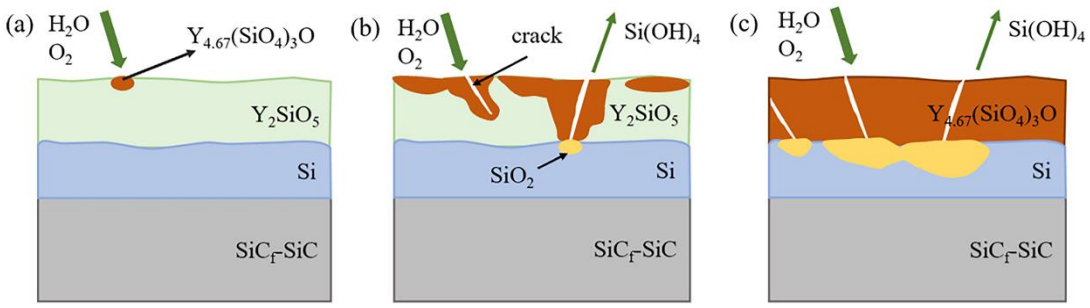

Fig. 4 Recession mechanism of Si/Y_2SiO_5 TEBC corroded in water vapor environment at (a) initial, (b) middle and (c) late stage

The Si/Y_2SiO_5 coated SiC_f/SiC sample is taken out from tube furnace every 10 hours to measure the variation of weight and flaking condition. After measuring, the sample is put back into tube furnace for next testing rotation. The take-out and put-back process during test accompany with great temperature change which will introduce great stress into Si/Y_2SiO_5 TEBC due to the different CTE between Y_2SiO_5 top layer and bond layer. With the influence of stress, a small number of micro-cracks in Y_2SiO_5 top layer will get wider and longer. Besides, the new cracks initiate as test continuing. Although oxygen permeability in Y_2SiO_5 is low, there are still small amount of oxygen penetrate through the top layer in the form oxygen ion. The molecular oxygen can also arrive at the interface between top layer and bond layer along the generated cracks. The oxygen ion and the oxygen molecule will react with silicon bond layer, leading to the formation of silica. Silica is also known as TGO. Not only oxygen, but also water vapor can penetrate through the top layer along the cracks. The water vapor reacts with TGO to form the volatile $Si(OH)_4$ as shown in Fig. 4(b). The weight gain caused by the oxidation of bond layer and the weight loss caused by the volatilization of $Si(OH)_4$ cancel each other out. So, the mass change versus time curve still keeps flat without obvious fluctuation before accumulated corrosion time extending to 193 hours. In short, although extension of cracks and the corrosion of bond layer happen, there is little impact on the total function of Si/Y_2SiO_5 coating. The Si/Y_2SiO_5 still efficiently isolates the SiC_f/SiC substrate from water vapor.

When corrosion test continued for over 193 hours, the generated longitudinal and transverse cracks intersect with each other, forming a connected three-dimensional crack network. The high temperature water vapor and oxygen get much easier to arrive at the bond layer. The severer oxidation of bond layer and volatilization of

$Si(OH)_4$ happen which deteriorates the bonding strength between top layer and bond layer. Part of Y_2SiO_5 layer peels off under the influence of stress. So, the mass change verses time curve dramatically drops down when corrosion time extend to 205 hours. Besides, during the long period of corrosion test, Y_2SiO_5 react with TGO to form $Y_{4.67}(SiO_4)_3O$ which is the reason why a large number of $Y_{4.67}(SiO_4)_3O$ can be detected after corrosion test. So, as shown in Fig. 4(c) the proportion of Y_2SiO_5 decreases and the proportion of $Y_{4.67}(SiO_4)_3O$ increases as the water vapor corrosion test continues.

3.3 Changing of Si/Y_2SiO_5 TEBC after CMAS corrosion

Fig. 5 (a)~Fig. 5(d) display the cross-section microstructure of Si/Y_2SiO_5 TEBC corroded by CMAS at 1300℃ for 30 min, 1 hour, 2.5 hour and 4 hours, respectively. It can be seen from Fig. 5 that there is a dense reaction zone between molten CMAS and Y_2SiO_5 top layer no matter how long the reaction continues. The thickness of reaction zone gets larger as the reaction time goes on.

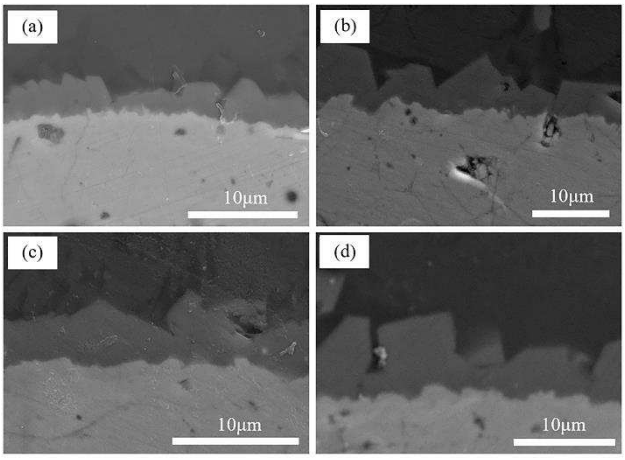

Fig. 5 Cross-section microstructure of Si/Y_2SiO_5 TEBC corroded by CMAS at 1300 ℃ for (a) 30 min, (b) 1 h, (c) 2.5 h, (d) 4h

Fig. 6 displays the EDS linear scan result of the cross section of Si/Y_2SiO_5 TEBC

after 4 hours' CMAS corrosion. There is no doubt that melted CMAS is rich in Ca, Mg, Al, Si and almost no Y can be detected. The reaction zone is also rich in Ca and Si. But the proportions of Mg and Al dramatically drop in reaction zone. There is a slightly increase of the amount of Y in reaction zone. In Y_2SiO_5 layer, the amount of Y rapidly increases but the amount of Ca decreases obviously. The amount of Si also decreases to a certain degree in Y_2SiO_5 layer.

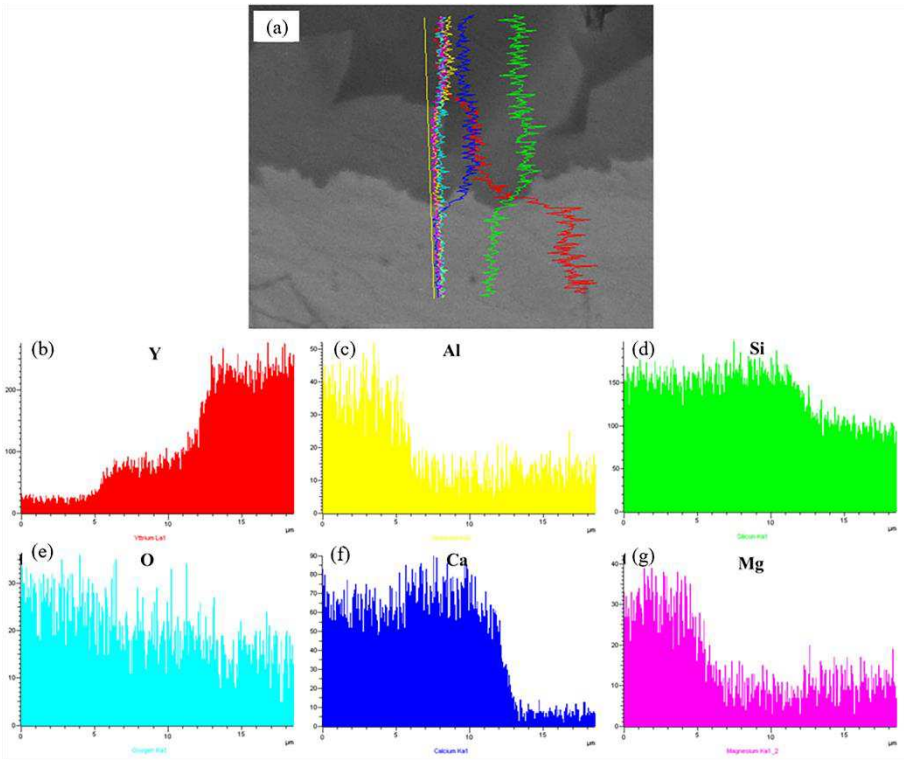

Fig. 6 EDS linear scan results of cross-section of Si/Y_2SiO_5 TEBC after CMAS corrosion at 1300 ℃ for 4 h (a) overall scanning result, (b) Y, (c) Al, (d) Si, (e) O, (f) Ca, (g) Mg

It can be summarized from the variation of element proportion shown in Fig. 6 that Ca and Si in CMAS continuously permeate into Y_2SiO_5, leading to the formation of reaction zone between melted CMAS and Y_2SiO_5. And this reaction zone can effectively stop the mutual diffusion of elements in CMAS and Y_2SiO_5. So, Y is not capable to diffuse into the reaction zone and CMAS layer and Mg and Al only be

detected in CMAS layer.

Fig. 7 displays the phase composition of the mixture of Y_2SiO_5 and CMAS powders as a weight ratio of 1:1 after heating at 1300℃ for 30 min and 4 hours, respectively. It can be seen from Fig. 7 (a) that after corroding for 30 min at 1300 ℃, $Y_{4.67}(SiO_4)_3O$ and $Ca_3Y_2(Si_3O_9)_2$ can be detected from the mixture of CMAS and Y_2SiO_5 powders. The content of $Y_{4.67}(SiO_4)_3O$ is higher than $Ca_3Y_2(Si_3O_9)_2$. At the beginning of CMAS corrosion test, part of SiO_2 in CMAS react with Y_2O_3 in Y_2SiO_5, leading to the formation of $Y_{4.67}(SiO_4)_3O$. Besides, the remaining SiO_2 and CaO in CMAS react with Y_2SiO_5 to form a small number of $Ca_3Y_2(Si_3O_9)_2$. The reaction equation mentioned above are described as follows:

$$2.335Y_2O_3(s)+3SiO_2 \rightarrow Y_{4.67}(SiO_4)_3O \quad (1)$$

$$3CaO+5SiO_2+Y_2SiO_5 \rightarrow Ca_3Y_2(Si_3O_9)_2 \quad (2)$$

When mixture of CMAS and Y_2SiO_5 powders is kept at 1300 ℃ for 4 hours, a large quantity of $Ca_4Y_6O(SiO_4)_6$ and small amount of $Ca_3Y_2(Si_3O_9)_2$ are created as shown in Fig. 7. As reaction time is prolonged, large amount of CaO and SiO_2 are consumed. The remaining small amount of CaO and SiO_2 react with Y_2SiO_5 to form the $Ca_4Y_6O(SiO_4)_6$. The reaction equation is described as follow:

$$4CaO+3SiO_2+3Y_2SiO_5 \rightarrow Ca_4Y_6O(SiO_4)_6 \quad (3)$$

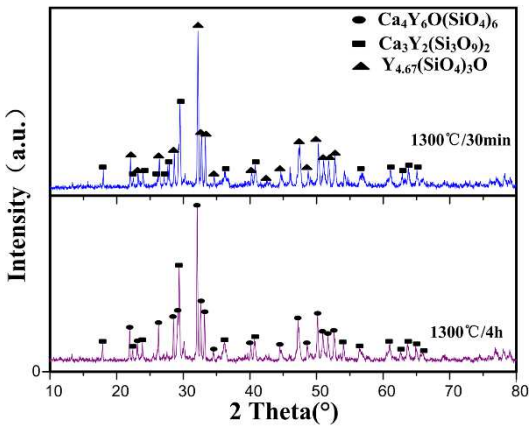

Fig. 7 Phase composition of the mixture of Y_2SiO_5 and CMAS powders

after keeping at 1300 ℃ for (a) 30 min and (b) 4 h

3.4 Reaction kinetics between CMAS and Si/Y_2SiO_5 coatings

Table 2 lists the thickness of reaction zone when Si/Y_2SiO_5 TEBC were corroded at 1200 ℃, 1250℃ and 1300 ℃ for different times. It can be found from Table 2 that at the same reaction temperature, as reaction time is prolonged, the reaction zone gets thicker. The thickness of reaction zone also increases with reaction temperature when corrosion time is same.

Table 2 The thickness of reaction zone formed with different corrosion temperature and time.

Reaction time, min	Thickness of reaction zone, μm		
	1200℃	1250℃	1300℃
15	0.238	0.575	2.31
90	0.31	1.239	3.66
150	0.36	1.529	4.31
240	0.4	1.848	5.15

Fig. 8 plots the thickness of reaction zone as a function of square root of oxidation time. Growth of the reaction zone seems to obey the parabolic law:

$$y=kt^{1/2}+b \quad (4)$$

Where y is the thickness of reaction zone, t is the oxidation time, k is the reaction rate constant, b is constant. Fitting process is conducted on thickness data listed in Table 2. According to the fitting result, the reaction rate constant at 1200℃, 1250℃ and 1300 ℃ are $0.1466\mu mh^{-1/2}$, $0.8425\mu mh^{-1/2}$ and $1.9963\mu mh^{-1/2}$, respectively. The reaction rate constant represents the growth rate of reaction zone at different temperature. When CMAS corrosion test is conducted at 1200 ℃, the growth rate of

reaction zone is very slow. As reaction temperature raising to 1250 ℃, the growth rate of reaction zone increases more than four-fold compare with that at 1200 ℃. When corrosion temperature continues to raise to 1300 ℃, thickness of reaction zone will dramatically increase more than twelve-fold compare with that at 1200 ℃.

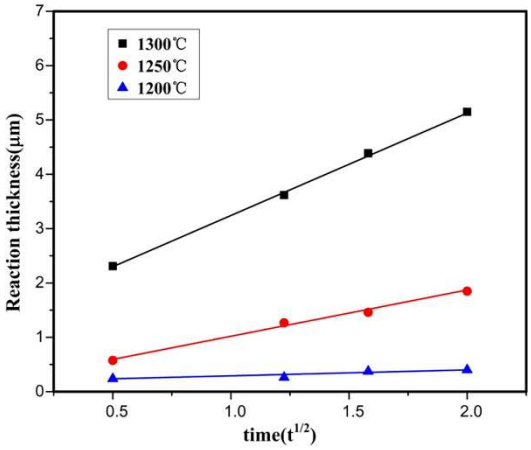

Fig. 8 Thickness of reaction zone as a function of square root of oxidation time

The obtained reaction rate constants at elevated temperature are plotted in Fig. 9. The apparent activation energy for the reaction between CMAS and Y_2SiO_5 layer can be calculated using Arrhenius formula as follow:

$$k=k_0 \exp(-E/2RT) \quad (5)$$

Where E is apparent activation energy for CMAS corrosion test, R is the ideal gas constant, T is temperature of CMAS corrosion test.

The natural logarithm of equation 5 is shown as follow:

$$\ln k - \ln k_0 = -E/2RT \quad (6)$$

According to the fitting result shown in Fig. 9, the relationship between the natural logarithm of reaction rate constant and reciprocal temperature obeys linear relation. The slope of fitting line represents the apparent activation energy for CMAS corrosion, which is calculated to be 713.749k J/mol.

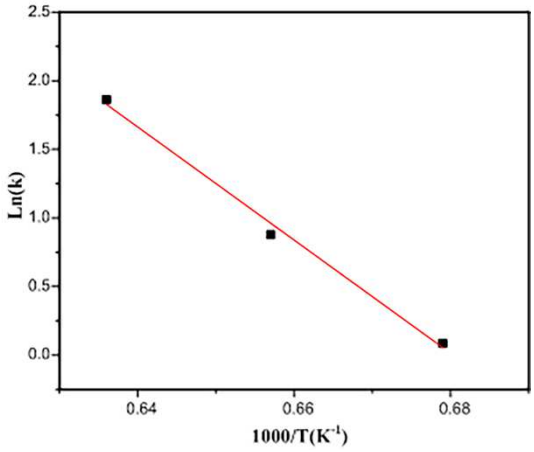

Fig. 9 Natural logarithm of reaction rate constant as a function of the inverse of temperature

4. Conclusions

Si/Y_2SiO_5 coated SiC_f/SiC were corroded by high temperature water vapor and CMAS in this research. The Si/Y_2SiO_5 TEBC can effectively separate SiC_f/SiC substrate from water vapor at 1300 ℃ for over 205 hours. After 250 hours' water vapor corrosion, the majority of Y_2SiO_5 have transformed into $Y_{4.67}(SiO_4)_3O$ because of the reaction between Y_2SiO_5 and TGO. With the influence of TGO and cracks caused by stress, part of Y_2SiO_5 top layer peels off along the TGO, causing the failure of Si/Y_2SiO_5 TEBC. The melted CMAS permeates into the Y_2SiO_5 top layer, leading to the formation of $Ca_4Y_6O(SiO_4)_6$ and $Ca_3Y_2(Si_3O_9)_2$ in reaction zone ultimately. The $Y_{4.67}(SiO_4)_3O$ is intermediates as test is executed at high temperature. The apparent activation energy of reaction between CMAS and Y_2SiO_5 is calculated to be 713.749k J/mol, which can be used to predict the reaction degree of CMAS corroding Y_2SiO_5 when corrosion temperature in the 1200 ~1300 ℃ temperature range. Overall, the findings obtained from this research are beneficial for screening the appropriate materials used for TEBC to protect Si-based CMC from high temperature water vapor

and CMAS corrosion.

References

[1] B.T. Richards, H.N.G. Wadley, Plasma spray deposition of tri-layer environmental barrier coatings, J. Eur. Ceram. Soc. 34 (2014) 3069-3083. http://doi.org/10.1016/j.jeurceramsoc.2014.04.027.

[2] N. Rohbeck, P. Morrell, P. Xiao, Degradation of ytterbium disilicate environmental barrier coatings in high temperature steam atmosphere, J. Eur. Ceram. Soc. 39 (2019) 3153-3163. http://doi.org/10.1016/j.jeurceramsoc.2019.04.034.

[3] E.N. Dayi, N. Al Nasiri, Diffusion study of rare-earth oxides into silica layer for environmental barrier coating applications, J. Eur. Ceram. Soc. 39 (2019) 4216-4222. http://doi.org/10.1016/j.jeurceramsoc.2019.05.026.

[4] S. Fujii, A. Ioki, T. Yokoi, Role of phonons on phase stabilization of $RE_2Si_2O_7$ over wide temperature range (RE = Yb, Gd), J. Eur. Ceram. Soc. 40 (2020) 780-788. http://doi.org/10.1016/j.jeurceramsoc.2019.10.060.

[5] A.V. Plyasunov, A.S. Zyubin, T.S. Zyubina, Thermodynamic properties of $Si(OH)_4(g)$ based on combined experimental and quantum chemistry data, J. Am. Ceram. Soc. 101 (2018) 4921-4926. http://doi.org/10.1111/jace.15922.

[6] B.T. Richards, K.A. Young, F. de Francqueville, Response of ytterbium disilicate-silicon environmental barrier coatings to thermal cycling in water vapor, Acta Mater. 106 (2016) 1-14. http://doi.org/10.1016/j.actamat.2015.12.053.

[7] K.N. Lee, D.S. Fox, N.P. Bansal, Rare earth silicate environmental barrier coatings for SiC/SiC composites and Si_3N_4 ceramics, J. Eur. Ceram. Soc. 25 (2005) 1705-1715. http://doi.org/10.1016/j.jeurceramsoc.2004.12.013.

[8] A.J. Fernández-Carrión, M. Allix, A.I. Becerro, Thermal expansion of rare-earth pyrosilicates, J. Am. Ceram. Soc. 96 (2013) 2298-2305.

http://doi.org/10.1111/jace.12388.

[9] Z. Tian, L. Zheng, W. Jiemin, Theoretical and experimental determination of the major thermo-mechanical properties of RE_2SiO_5 (RE=Tb, Dy, Ho, Er, Tm, Yb,Lu, and Y) for environmental and thermal barrier coating, J. Eur. Ceram. Soc. 36 (201) 189-202. http://doi.org/10.1016/j.jeurceramsoc.2015.09.013.

[10] Z. Sun, J. Wang, M. Li, Mechanical properties and damage tolerance of Y_2SiO_5, J. Eur. Ceram. Soc. 28 (2008) 2895-2901. http://doi.org/10.1016/j.jeurceramsoc.2008.04.029.

[11] Z. Sun, M. Li, Y. Zhou, Thermal properties of single-phase Y_2SiO_5, J. Eur. Ceram. Soc. 29 (2009) 551-557. http://doi.org/10.1016/j.jeurceramsoc.2008.07.026.

[12] Y. Ogura, M. Kondo, T. Morimoto, Oxygen permeability of Y_2SiO_5, Mater. Trans. 42 (2001) 1124-1130. http://doi.org/10.2320/matertrans.42.1124.

[13] J. Han, Y. Wang, R. Liu, Study on water vapor corrosion resistance of rare earth monosilicates RE_2SiO_5 (RE = Lu, Yb, Tm, Er, Ho, Dy, Y, and Sc) from first-principles calculations, Heliyon. 4 (2018) e00857. http://doi.org/10.1016/j.heliyon.2018.e00857.

[14] B. Ywa, A. Yn, Z.A. Xin, Water vapor corrosion behaviors of plasma sprayed RE_2SiO_5 (RE = Gd, Y, Er) coatings, Corros. Sci. 167 (2020) http://doi.org/10.1016/j.corsci.2020.108529.

[15] N. Al Nasiri, N. Patra, D.D. Jayaseelan, Water vapour corrosion of rare earth monosilicates for environmental barrier coating application, Ceram. Int. 43 (2017) 7393-7400. http://doi.org/10.1016/j.ceramint.2017.02.123.

[16] Z. Tian, C. Lin, L. Zheng, Defect-mediated multiple-enhancement of phonon scattering and decrement of thermal conductivity in $(Y_xYb_{1-x})_2SiO_5$ solid solution, Acta Mater. 144 (2018) 292-304. http://doi.org/10.1016/j.actamat.2017.10.064.

[17] B.K. Jang, F.J. Feng, K.S. Lee, Thermal behavior and mechanical properties of

Y_2SiO_5 environmental barrier coatings after isothermal heat treatment, Surf. Coat. Tech. (2016) 24-30. http://doi.org/10.1016/j.surfcoat.2016.09.088.

[18] Z. Tian, X. Ren, Y. Lei, Corrosion of $RE_2Si_2O_7$ (RE=Y, Yb, and Lu) environmental barrier coating materials by molten calcium-magnesium-alumino-silicate glass at high temperatures, J. Eur. Ceram. Soc. 39 (2019) 4245-4254. http://doi.org/10.1016/j.jeurceramsoc.2019.05.036.

[19] E. Garcia, H. Lee, S. Sampath, Phase and microstructure evolution in plasma sprayed $Yb_2Si_2O_7$ coatings, J. Eur. Ceram. Soc. 39 (2019) 1477-1486. http://doi.org/10.1016/j.jeurceramsoc.2018.11.018.

[20] Z. Tian, L. Zheng, W. Hu, Tunable properties of $(Ho_xY_{1-x})_2SiO_5$ as damage self-monitoring environmental/thermal barrier coating candidates, Sci. Rep.-UK. 9 (2019) http://doi.org/10.1038/s41598-018-36883-2.

[21] L. Liu, W. Zheng, Z. Ma, Study on water corrosion behavior of $ZrSiO_4$ materials, J. Adv. Ceram. 7 (2018) 336-342. http://doi.org/10.1007/s40145-018-0283-3.